Adaptive Learning on Time Series: Method and Financial Applications

Parley Ruogu Yang^{a, b, †}, Ryan Lucas^{b, c}, and Camilla Schelpe^b

^aFaculty of Mathematics, University of Cambridge ^bOptimal Portfolio Research Group ^cUniversity College Dublin [†]Correspondent: ry266@cam.ac.uk

First Version : 21 Oct 2021 Current Version : 16 Nov 2021 Most Recent Version : Click Here

ABSTRACT

We formally introduce a time series statistical learning method, called Adaptive Learning, capable of handling model selection, out-of-sample forecasting and interpretation in a noisy environment. Through simulation studies we demonstrate that the method can outperform traditional model selection techniques such as AIC and BIC in the presence of regime-switching, as well as facilitating window size determination when the Data Generating Process is time-varying. Empirically, we use the method to forecast S&P 500 returns across multiple forecast horizons, employing information from the VIX Curve and the Yield Curve. We find that Adaptive Learning models are generally on par with, if not better than, the best of the parametric models a posteriori, evaluated in terms of MSE, while also outperforming under cross validation. We present a financial application of the learning results and an interpretation of the learning regime during the 2020 market crash. These studies can be extended in both a statistical direction and in terms of financial applications.

Key words: Time Series, Forecasting Methods, Model Selection, Model Evaluation, Finance

ACKNOWLEDGEMENT

All authors would like to acknowledge Raena McElwee (OPRG & UCD) for assisting with the research: visualisation and literature discussions in particular.

1 Introduction

At any given point in time, we can observe the data generated previously and study the temporal distribution of the Data Generating Process (DGP). Forecasting then attempts to predict the future, conditional on historical observations and the knowledge obtained from studying the DGP. In this paper we formally study the Adaptive Learning (AL) method, founded in the intersection between Statistical Learning Theory (SLT) and time series.

The AL method was first introduced in Yang (2020), which finds empirical success in forecasting US GDP growth using the Yield Curve. The methods fits in the application of modern SLT and financial econometric literature. In terms of the learning aspect, as recently reviewed by the Alan Turing Institute (Ostmann and Dorobantu 2021), the good statistical learning methods, more broadly Artificial Intelligence, should yield logical information within the learning regime: system design and evaluation for instance, to all relevant stakeholders. Coulombe et al. (2020) and Coulombe (2020) draw good examples on how such methods can be used in the macroeconomics. Amongst many other literature, Taylor and Yu (2016) and Crook et al. (2020) have demonstrated how financial metrics can be useful as a contextual evaluation for modern statistical learning models, with extension to financial risk management. Discussions on Sharpe Ratio as a statistical measurement can be further traced to Lo (2002) and Benhamou et al. (2019), where this fits in a financial time series context, on top of its original use as a tool for portfolio evaluation in finance.

There are three motivating fields of literature on the relevant statistical methods: one in modern time series as concerned by econometricians, e.g. Harvey (2013), another in the change points detection as has been developed by mathematicians and engineers (Liu, Gao, and Samworth 2021), the other in robust statistics and penalisations (Huber and Ronchetti 2009; Spokoiny 2017), where the design of loss function motivates some set-ups of the AL. Model selection in a change point time series regime sits in conjunction with these three fields: in a stable time series without a change point, AIC (Akaike 1974), BIC (Schwarz 1978), and other information criteria can reasonably outperform as these criteria were developed on purpose. However, if we consider a time post-change points when we model based on data observed in the past, then the models and associated evaluation using data before the change point can be thought as contaminated data, which relates to robust statistics, and the suitability of traditional evaluation methods becomes a question. Recent attempts on this problem merges cross validation and the information criteria (Yang 2007; Zou, Wang, and Li 2020). The AL is another attempt at model selection, as Yang (2021) demonstrated the possibility for AL to select lags based on the unique time-series information that forecasting yields. On top of that, the financial evaluation in a change point or contaminated environment may differ hugely to the traditional metrics, e.g. MSE, and may be more robust instead.

On the empirical side, there is a large body of existing literature linking the Yield Curve to future economic growth and many other important macroeconomic variables (Estrella and Mishkin 1996; De Pace 2013), especially prior to the downturn of the macroeconomy. Likewise, the VIX Curve has become widely recognised amongst the practitioner community as an important signal for the future state of the stock market (Fassas 2012; Fassas and Hourvouliades 2019). The upper panel of Figure 1 shows the state of these relationships on 24 Feb 2020, demonstrating that inversions of both curves can signal a downturn in the stock market. We further this analysis in subsection 4.3, providing a case study on the 2020 market crash. The general relationship over the empirical period studied is illustrated in the lower panels of Figure 1, and corroborates with the nature of the relationships described elsewhere in the literature. Still, despite numerous studies suggesting the existence of a relationship, a detailed forecasting study has yet to be conducted; neither has a study been done using non-traditional evaluation metrics and statistical learning techniques.

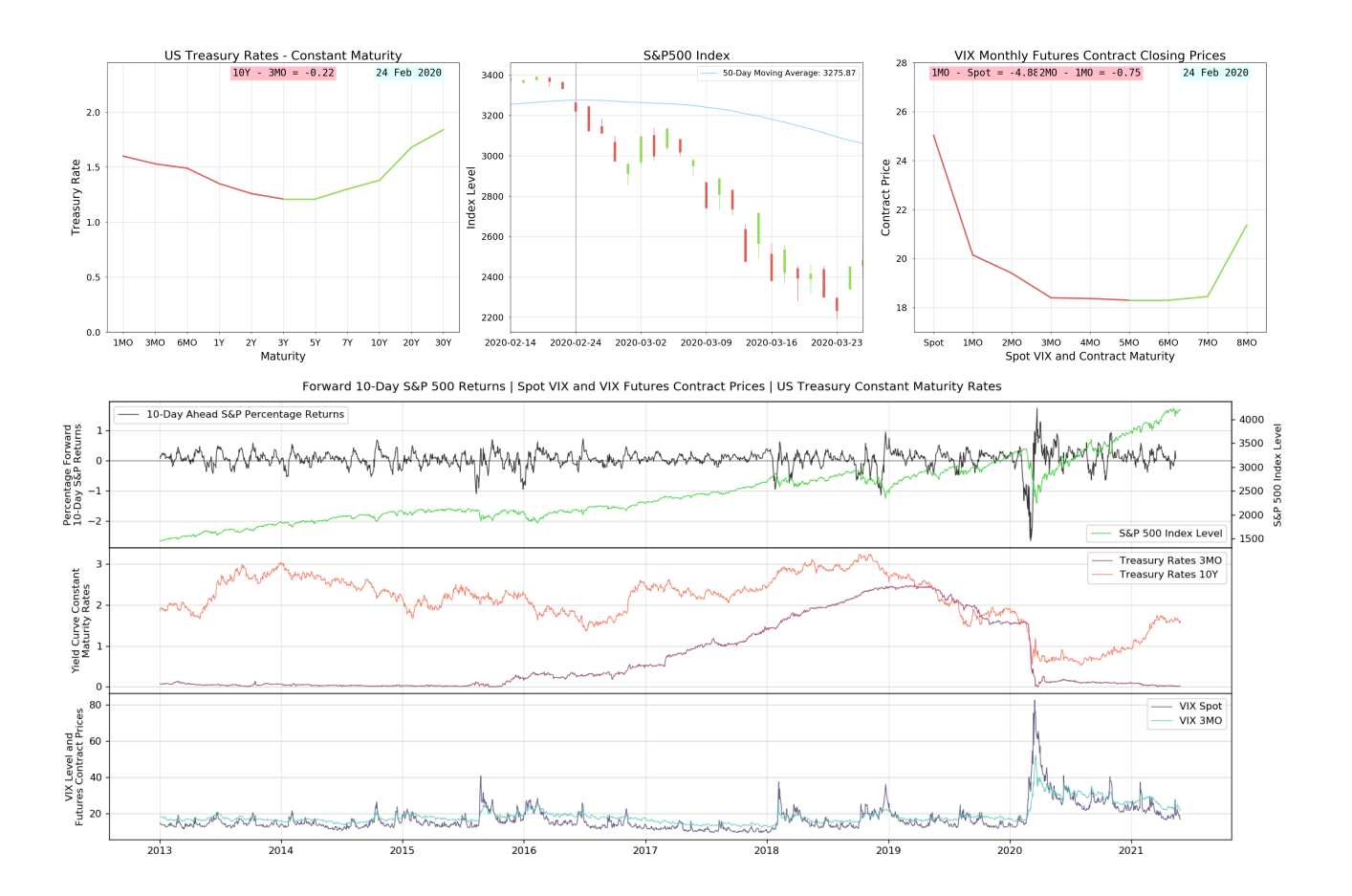


Figure 1: The upper panel displays the Yield Curve (left) and VIX Curve (right) alongside the price of the S&P 500 index (centre) during the pandemic-induced market contraction of 2020. An inversion in these curves preceded the collapse of the index. The lower three panels describe the general relationships over the full dataset, which can at times be highly synchronous. The dynamic plots across time can be found at https://optimalportfolio.github.io/subpages/Videos.html

Our contribution to the literature is three-fold. On the methodological side, we provide a formal background to the AL method, and demonstrate how various loss functions used in modern statistics can be incorporated in the learning process specific to time series. Moreover, by demonstrating the value of AL as a model selection technique using both traditional evaluation metrics (e.g. MSE) and non-traditional ones (e.g. Sharpe Ratio, Maximum Drawdown), we provide a proof-of-concept for SLT in the domain of financial time series. Finally, this paper also contributes to the macroeconomic and financial literature by demonstrating that improved forecasting of the S&P 500 can be achieved by incorporating explanatory variables derived from the VIX and Yield Curves, particularly during the 2020 crash.

As a brief outline to this paper, in section 2 we introduce the background of time series and describe the method of AL in detail. In section 3 we illustrate the performance in different simulated DGPs, and discuss both traditional and financial evaluation metrics. We move on to an empirical forecasting application of the method in section 4 and provide a detailed case study of the 2020 financial crash. The findings of the paper are summarised and discussed in section 5. Appendix A contains further technical details, including common notation used in this paper. We would like to highlight that the use of uppercase letters, e.g. Y_t , is reserved for discussions on the underlying DGP of a random variable Y at time t. Lowercase letters are used when the observed value is discussed, e.g. y_t for the observed value of Y at time t.

¹ On some occasions, capital letters also used to denote a set. This is distinguished clearly in the context.

2 Methodologies

2.1 Background and Motivation

2.1.1 Setup of Time Series

Denote $y_t \in \mathbb{R}$ and $x_t \in \mathbb{R}^d$ as the observed value of the dependent random variable Y and explanatory random variable X, respectively, at a discrete time t. In this paper, we focus on a parametric model where we assume $y_t \sim P_{Y|X}^t(\cdot|x_t;\theta)$, that is, the observed dependent value is drawn from an unknown conditional distribution $P_{Y|X}^t$ parameterised by θ .

The key tasks of time series statistics are as follows:

- Estimation: this may be viewed as, narrowly, parametric estimation at time t, to estimate the unknown conditional distribution $P^t_{Y|X}(\cdot|\cdot;\theta)$ using the data we have. From this, we compute $\hat{\theta}_t$ and eventually the estimated distribution $P^t_{Y|X}(\cdot|\cdot;\hat{\theta}_t)$. These depend on the methodology of estimation and data Ω_t .
- Point forecasting²: At time t we have observations from time index 1 to t, hence denote the dataset as $\Omega_t := \{(y_\tau, x_\tau) : \tau \in [t]\}$. Given a forecast horizon $k \in \mathbb{N}$, we would like to produce a point forecast of Y at the time index t + k, conditional on the observed information. This can be denoted as

$$\hat{y}_{t+k|t} := \mathbb{E}[Y_{t+k}|\Omega_t, \hat{\theta}_t(\Omega_t)] \tag{1}$$

There are, however, numerous unique problems encountered with time series data: mainly due to the fact that the distribution, or more generally, the structure of the DGP can be time-varying, hence causing problems in estimation and forecasting. We discuss three aspects below.

The first is time-varying distribution: at some time t, we face $P_{Y|X}^t \neq P_{Y|X}^{t+1}$. This may be at a functional level, e.g. the DGP changes from an AR(1) to AR(2), or may be at a parameter level, e.g. for the same AR(1) process, the parameter varies, also known as 'time-varying parameter' in the econometric literature. In subsection 3.2, we study this more closely to demonstrate the improvement AL makes to the forecasting of various simulated data sets with change points, in both a general time series framework and a specific financial stochastic process. See Figure 2 for the simulated examples.

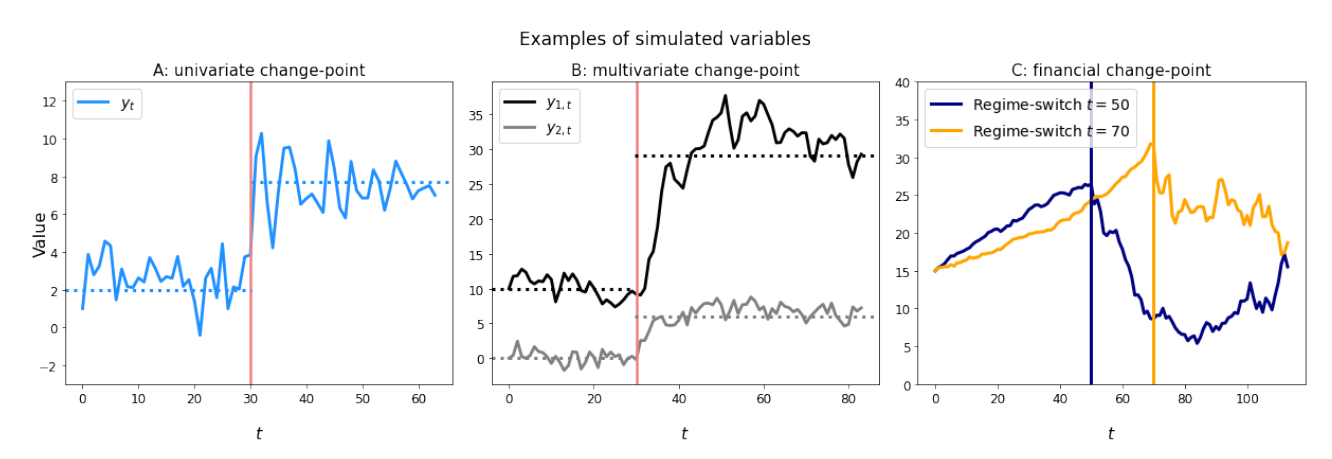


Figure 2: Samples of simulated data drawn from systems A, B and C as studied in subsection 3.2

The second is on modelling and forecasts: there can be systems of equations where insufficient information is given for forecasts to be generated. For instance, consider the estimation equation $y_t = \beta x_t + \varepsilon_t$, then the forecast $\hat{y}_{t+1|t}$ cannot be made, as the future state x_{t+1} is not available

² More general forms of forecasting, e.g. interval forecasting or distributional forecasting are not introduced here, as they are not part of the theme of this paper.

conditional on Ω_t . To compute the forecast, a typical solution is vector time series models, such as VAR, but these increase the size of the parameter space. An alternative solution which does not boost the parameter space is to estimate the lagged relationship $y_t = \beta x_{t-1} + \varepsilon_t$, but that may give biased estimation or even suffer serially correlated error, depending on the original DGP. So, there are always a wide choice of models, not to mention the non-linear approximations such as by Neural Networks and more sophisticated learning algorithms. In this paper, AL is proposed in light of the model selection problems, which can be more complicated in time series as the variety both in the models and estimation methods, even just for the linear ones, can be huge. Further modelling and estimation topics are discussed in section 3 and section 4.

With the above two problems that are unique to time series, the third problem arises as to the appropriateness of evaluation methods, especially in light of time-varying distributions. As could be observed in many empirical datasets such as Figure 1, the distribution of the data may vary drastically, which can create problems for ordinary evaluation techniques, e.g. MSE. Here, we focus on financial time series and attempt to use financial evaluation metrics to aid traditional statistical evaluation of models. Our key findings, both through simulation and empirical data, is that the relationship between MSE and financial metrics is time-varying, and can be very weak (e.g. see Figure 4) depending on the time-varying distributions.

2.1.2 The Value of Forecasting

Here, we study an interesting phenomenon of causal time series to appreciate the value of the forecasting exploited in AL. From Shumway and Stoffer (2017), a time series Y_t is causal if, for all $t \in \mathbb{N}$,

$$Y_t = \mu + \sum_{j=0}^{\infty} \psi_j \varepsilon_{t-j} \tag{2}$$

where $\psi := (\psi_j)_{j=0}^{\infty}$, $\psi \in \mathcal{L}^1(\mathbb{N})$. Writing the k-step-ahead forecast conditional on true parameters as $y_{t+k|t} := \mathbb{E}[Y_{t+k}|\Omega_t, \theta]$, then we have

$$y_{t+k|t} = \mu + \sum_{j=k}^{\infty} \psi_j \varepsilon_{t+k-j} = y_{t+k} - \sum_{j=0}^{k-1} \psi_j \varepsilon_{t+k-j}$$
(3)

Notice that we never have access to $y_{t+k|t}$ — it is the forecast made based on the true parameters, which are always unknown to us. The forecast we obtain is $\hat{y}_{t+k|t}$ based on the estimated parameters as was introduced previously. Hence, if we were to compare the forecasts against the observed value, we have

$$y_{t+k} - \hat{y}_{t+k|t} = (y_{t+k|t} - \hat{y}_{t+k|t}) + (y_{t+k} - y_{t+k|t})$$

$$\tag{4}$$

$$= (y_{t+k|t} - \hat{y}_{t+k|t}) + \sum_{j=0}^{k-1} \psi_j \varepsilon_{t+k-j}$$
 (5)

Equation 4 can be understood as a classical decomposition for validation error, where the first term on the right is the estimation error, reducible by a better modelling and estimation techniques, whereas the second term is the natural noise in the DGP, irreducible by the model or estimation. Equation 5 is a consequence of Equation 3, which is due to the structure of causal time series (Equation 2). From the above, we see that past forecasts yield information on the goodness of the model. While this is the concept of "cross validation" in SLT, it is harder to manage such a validation exercise in time series due to their unique temporal structure. The observation in Equation 5 clarifies this for the class of causal time series. In particular, the larger the k, more natural noises are added, influencing the

quality of forecast evaluation. As an easy example, we observe a stationary AR(1) process:

$$Y_t = c + \phi Y_{t-1} + \varepsilon_t \tag{6}$$

where $\phi \in (-1,1)$. ³ Now, observe

$$y_{t+k} - \hat{y}_{t+k|t} = \left(c\left(\frac{1-\phi^k}{1-\phi}\right) - \hat{c}_t\left(\frac{1-\hat{\phi}_t^k}{1-\hat{\phi}_t}\right) + (\phi^k - \hat{\phi}_t^k)y_t\right) + \sum_{j=0}^{k-1} \phi^j \varepsilon_{t+k-j}$$
(7)

The bracketed terms are due to the estimation error, whereas the last term is natural noise. While the bracketed terms contain information about the reducible errors due to estimation $(\hat{c}_t, \hat{\phi}_t)$, there are decaying extra noise terms associated with the information $\sum_{j=0}^{k-1} \phi^j \varepsilon_{t+k-j}$.

2.2 Definition of AL

We start by formalising how a forecast is computed. We assume that we are at time t, aiming to make a forecast k-step ahead, and that Ω_t is naturally available. First, we need to have a functional specification h, the model that dictates the relationship between dependent and independent variables. Write the **collection of functional specifications** as H. Now, given a functional specification, we have a parametric set $\Theta(h)$, e.g. in the case of h = AR(1), $\Theta(AR(1))$ is a proper subset of \mathbb{R}^2 .⁴ An estimation technique is defined as a map which takes the parametric set and temporal data as input, and outputs the estimated statistics, mathematically $\Xi_h(\Theta(h), \Omega_t) = \hat{\theta}_t(h) \in \Theta(h)$. We note, as discussed previously, that a functional specification can have many methods of estimation, denoted I(h) as an index set. A forecast can be computed by first determining $\hat{\theta}_t(h)$ and subsequently $\hat{y}_{t+k|t}(h,\Xi_h)$ as per the standard definition (Equation 1). Finally, we introduce a loss function ℓ that takes the generated forecast based on (h,Ξ_h) , and compares to the observed true value, thereafter producing the loss associated with a particular model and estimation technique pair.

With the above notation, we are able to introduce AL concisely. An AL specification is a quadruple $(\ell, H^{AL}, H, \{\Xi_{h,i}\}_{i \in I(h), h \in H})$ such that, at time t:

- 1. The set of functional specifications for AL, denoted H^{AL} , should enable the AL forecasts to be adapted to the constituent models: $H^{AL} \supseteq H$
- 2. $\forall h \in H, I(h) \neq \emptyset$ and $\forall i \in I(h), \Xi_{h,i} : \Theta(h) \times \Omega_t \mapsto \hat{\theta}_t(h)$ is well-defined.
- 3. $\forall h \in H, \, \forall i \in I(h), \, \forall \tilde{k} \in [k], \, \text{the forecast } \hat{y}_{t+\tilde{k}|t}(h,\Xi_{h,i}) \text{ is well-defined.}$
- 4. Upon evaluating ℓ with the relevant information, $\hat{y}_{t+k|t}(h_t^{AL})$ and $h_t^{AL} \in H^{AL}$ are the outputs.

We note that the fourth condition is quite general: we further illustrate configurations of ℓ and introduce the method to compute $\hat{y}_{t+k|t}(h_t^{AL})$ below.

2.3 Key AL specifications

2.3.1 DMS

We first look at the case of $H^{AL} = H$, which is known as Dynamic Model Selection (DMS). The key here is to select the model at time t and adapt the forecast to the selected one. In particular, we use

$$\phi \in (-1,1) \iff \psi \in \mathcal{L}^1(\mathbb{N})$$

Therefore this parametric restriction is a necessary and sufficient one for Y_t to be causal.

We may observe, by reconciling between Equation 6 and Equation 2 that $\psi_j = \phi^j$ and hence

⁴ This may be arguable as to whether the variance estimator is counted towards the parametric set — here, we only count for the constant term and the autoregressive term(s) as they are the ones which contribute to the point forecasting. In the case of an AR(1), this gives 2 dimensions.

 ℓ to facilitate the evaluation of the 'goodness' of the model, therefore returning $\hat{y}_{t+k|t}(h^{AL})$.

Consider a v-sized window up to time t, $\{y_{\tau}\}_{\tau=t-v+1}^{t}$, and a given pair $(h, \Xi_{h,i})$. Based on the third condition in the definition of AL, we have $\hat{y}_{\tau|\tau-\tilde{k}}$ for all $\tau \in \{t-v-k+1,...,t-1,t\}$ and $\tilde{k} \in [k]$. Define $\mathbf{1}_{k} := (1,1,...,1,1) \in \mathbb{R}^{k}$ and $\hat{\mathbf{y}}_{\tau+k|\tau} := (\hat{y}_{\tau+k|\tau+k-1},\hat{y}_{\tau+k|\tau+k-2},...,\hat{y}_{\tau+k|\tau}) \in \mathbb{R}^{k}$. Now, define the formulations of ℓ as below:

$$\ell^{\text{Norm, single-valued}}(h, \Xi_{h,i}; \lambda, p) := \sum_{\tau = t - v + 1}^{t} \lambda^{t - \tau} |\hat{y}_{\tau|\tau - k} - y_{\tau}|^{p} \tag{8}$$

$$\ell^{\text{Norm, multi-valued}}(h, \Xi_{h,i}; \lambda, p) := \sum_{\tau = t - v + 1}^{t} \lambda^{t - \tau} ||\hat{\boldsymbol{y}}_{\tau|\tau - k} - y_{\tau} \boldsymbol{1}_{k}||_{p}^{p} \tag{9}$$

The associated parameters are $\lambda \in (0,1]$ and $p \in (0,\infty)$. While v is clearly a parameter as well, it is not being investigated in this paper, as $\lambda^{t-\tau}$ discounts the history in a way that controls the effective contribution of far history to the loss. For general intuition, we start by taking $\lambda = 1$ and $p \in \{1,2\}$, then Equation 8 is simply an MAE or MSE over the period. The smaller the λ , the more focused the learning is towards the recent history, and vice versa.

The key motivation behind Equation 9 is as follows. For $k \geq 2$, the term that differs from Equation 8 is $\hat{y}_{\tau|\tau-k} - y_{\tau} \mathbf{1}_k$. This is a vector containing information in a higher dimension than just the scalar $\hat{y}_{\tau|\tau-k} - y_{\tau}$. It additionally compares, for instance, $\hat{y}_{\tau|\tau-1}$ against the true value y_{τ} . We note that $\hat{y}_{\tau|\tau-1}$ uses information Ω_{t-1} which is more recent than the one used by $\hat{y}_{\tau|\tau-k}$, hence faces less noise and more contemporary information on the performance of model and estimation techniques, e.g. see Equation 5. A further study via an example is made in subsection 3.1.

Following the above configuration of the loss function, we find the pair which minimises the loss:

$$(h^*, \Xi_{h,i}^*) := \underset{(h,\Xi_{h,i}) \in \cup \{(h,\Xi_{h,i}) : i \in I(h), h \in H\}}{\arg \min} \ell(h, \Xi_{h,i})$$

$$(10)$$

AL then adapts to the selected model for forecasts: $\hat{y}_{t+k|t}(h_t^{AL}) = \hat{y}_{t+k|t}(h^*, \Xi_{h,i}^*)$. For a general algorithm for computing implementation, see algorithm 1.

Algorithm 1: AL implementation for DMS

Input: Data, desired forecasting index set T, and AL specifications

 $(\ell, H^{AL}, H, \{\Xi_{h,i}\}_{i \in I(h), h \in H})$ with v

Output: Forecasts $\{\hat{y}_{t+k|t}(h_t^{AL})\}_{t\in T}$ with the associated models $\{(h_t^{AL})\}_{t\in T}$

- 1. For $t \in T$, repeat:
 - (a) Evaluate ℓ given the information required. Then find $h^* \in H$ and $\Xi_{h,i}^*$ which minimises the loss.
 - (b) Obtain and store $\hat{y}_{t+k|t}(h_t^{AL}) := \hat{y}_{t+k|t}(h^*, \Xi_{h,i}^*)$ as the forecast

2.3.2 Ensemble

The other case is known as the Ensemble method where the AL forecasts take the form of a convex combination of the forecasts from H. Here, the AL models take place in a simplex $H^{AL} = \Delta(N)$ where $N := |\cup \{(h, \Xi_{h,i}) : i \in I(h), h \in H\}|$, which is the total number of estimation techniques across all models. Enumerate the set $\cup \{(h, \Xi_{h,i}) : i \in I(h), h \in H\}$ into [N] and align the associated forecasts to a N dimensional vector $\hat{y}_{t+k|t}^N$. Finally, for an element called ensemble weights $\delta_t \in \Delta(N)$, the AL adapts to the selected weights by the inner product: $\hat{y}_{t+k|t}(h^{AL}) = \langle \delta_t, \hat{y}_{t+k|t}^N \rangle$. It remains to introduce the method of determining the weight below.

We subsample the data points in the window v as follows. Consider a smaller window v_0 , and for each time $\tau \in \{t-v_0+1,...,t-1,t\}$, look back a window of v_1 , where $v_1=v-v_0$. Find the best model in the v_1 window up to each time τ . That is, for each τ , we proceed with the optimisation as per Equation 10. Allocate an equal weight of v_0^{-1} to the model selected. This then produces $\delta_t \in \Delta(N)$ as desired. See algorithm 2 for a general algorithm.

Algorithm 2: AL implementation for Ensemble

Input: Data, desired forecasting index set T, and AL specifications

 $(\ell, H^{AL}, H, \{\Xi_{h,i}\}_{i \in I(h), h \in H})$ with pair (v_0, v_1)

Output: Forecasts $\{\hat{y}_{t+k|t}(h_t^{AL})\}_{t\in T}$ with the associated models $\{(h_t^{AL})\}_{t\in T}$

- 1. Enumerate H to [N].
- 2. For $t \in T$, repeat:
 - (a) For $\tau \in \{t v_0 + 1, ..., t\}$, repeat:
 - i. Evaluate ℓ given the information required. Then find $h^* \in H$ and $\Xi_{h,i}^*$ which minimises the loss.
 - ii. Allocate a weight of v_0^{-1} to the minimiser
 - (b) Collect the weights δ_t and align the forecast vector $\hat{y}_{t+k|t}^N$
 - (c) Obtain and store $\hat{y}_{t+k|t}(h_t^{AL}) = \langle \delta_t, \hat{y}_{t+k|t}^N \rangle$ as the forecast

2.3.3 Huber Loss

As a remark, the generalised configuration of Equation 9 is

$$\ell^{\text{multi-valued}}(h, \Xi_{h,i}; \lambda, \ell^{\text{local}}) := \sum_{\tau = t - v + 1}^{t} \lambda^{t - \tau} \ell^{\text{local}}(\hat{\boldsymbol{y}}_{\tau | \tau - k}(h, \Xi_{h,i}), y_{\tau} \mathbf{1}_{k})$$
(11)

with $\ell^{\text{local}}(\cdot)$ taking different specifications at a local k-dimensional level. A combination of 1-norm and 2-norm, which may be robust to contaminated data, is the Huber loss. Recall that a Huber loss takes the form

$$Huber(x;c) := \begin{cases} cx - \frac{1}{2}c^2 & \text{if } x \ge c\\ \frac{1}{2}x^2 & \text{if } x < c \end{cases}$$
 (12)

For our local loss to take that, we could put ℓ^{local} as

$$\ell^{\text{Huber}}(\hat{\boldsymbol{y}}_{\tau|\tau-k}, y_{\tau} \mathbf{1}_k; \boldsymbol{c}) := \sum_{j=1}^k Huber(|\hat{y}_{\tau|\tau-j} - y_{\tau}|; c_j)$$
(13)

To determine the vector of parameters $\mathbf{c} := (c_1, ..., c_k)$, we can do so by selecting from the empirical quantiles of $\{|\hat{y}_{\tau|\tau-j}(h, \Xi_{h,i}) - y_{\tau}| : i \in I(h), h \in H\}$ and take it as c_j , for all $j \in [k]$.

2.3.4 Loss Comparing Against A Benchmark (MC)

From Equation 11, we may define ℓ^{local} to compare the norm loss of a model against a benchmark. To formalise this, denote (g, Ξ_q) as the desired benchmark, then define

$$\ell^{\text{MC}}(\hat{\boldsymbol{y}}_{\tau|\tau-k}, y_{\tau} \mathbf{1}_{k}; p, g, \Xi_{g}) := \frac{||\hat{\boldsymbol{y}}_{\tau|\tau-k}(h, \Xi_{h,i}) - y_{\tau} \mathbf{1}_{k}||_{p}^{p}}{||\hat{\boldsymbol{y}}_{\tau|\tau-k}(g, \Xi_{g}) - y_{\tau} \mathbf{1}_{k}||_{p}^{p}}$$
(14)

3 Simulation Studies

$3.1 \quad AR(1)$

We start with a simple example: consider an AR(1) process (Equation 6) and set the forecasting horizon k = 2. We fix $H = \{AR(1)\}$ and design two least square estimation techniques: one uses a window sized 10 (denoted Ξ_1) and another sized 20 (denoted Ξ_2) to determine the coefficients in the AR(1) process. We refer to these two (h,Ξ) pairs as fixed models, which the AL model chooses between at each timestep. For the ease of analysis, we assume the c term is known, so the only difference is the estimation of ϕ and σ^2 . Then the forecasting error can be written down as

$$y_t - \hat{y}_{t|t-1} = y_{t-1}(\phi - \hat{\phi}_{t-1}) + \varepsilon_t \tag{15}$$

$$y_{t} - \hat{y}_{t|t-2} = c(\phi - \hat{\phi}_{t-2}) + y_{t-2}(\phi^{2} - \hat{\phi}_{t-2}^{2}) + \phi \varepsilon_{t-1} + \varepsilon_{t}$$
(16)

We specify the loss function configurations in Equation 8 and Equation 9 with p=1 and v=1, thus λ does not matter. We notice that the single-valued loss function only compares $|y_t - \hat{y}_{t|t-2}|$ between Ξ_1 and Ξ_2 , while the multi-valued one compares $|y_t - \hat{y}_{t|t-2}| + |y_t - \hat{y}_{t|t-1}|$ between Ξ_1 and Ξ_2 , which means the loss is affected by $\hat{\phi}_{t-1}$ on top of $\hat{\phi}_{t-2}$.

For the simulated results, we fix $c = 1 - \phi$ and report the squared forecasting error at time t = 30 under different ϕ . This is reported in Table 1. Notice that between the two fixed models, in all cases Ξ_2 has a smaller forecasting error due to the improved stability that comes with a larger estimation window (in the case of a static DGP). We observe that for larger ϕ , AL offers much more competitive forecasts. It adapts to the model in accordance with the loss, and outputs a forecast which, as can be seen in the table, outperforms the forecasts from the individual fixed models on average. This phenomenon is more significant when ϕ is larger, which is most likely due to the irreducible forecasting error proportional to ε_t becoming less dominant. In terms of the multi-valued AL specifications: there is a clear out-performance compared to the single-valued loss, which corroborates the intuition explained above.

ϕ	single-valued AL	multi-valued AL	Ξ_1	Ξ_2
0.2	1.290	1.243	1.461	1.242
0.5	2.049	1.896	2.660	1.918
0.9	3.756	3.690	4.280	4.018
0.95	4.249	4.209	4.587	4.858

Table 1: Average MSE across 10000 simulated samples

3.2 Change Points

In this subsection, we study three different time series systems: two of which (A and B) are autoregressive processes and the other (C) is a stochastic process. In each system, we simulate a regime-switch to occur at defined change points. Examples of the simulated series are given in Figure 2. For each system, we fit a set of parametric models and AL models to the series, and make forecasts for the unseen simulated data. We study a total of 8 AL configurations, with technical details stated in subsection A.2. The abbreviations for single-valued (Equation 8) and multiple norm (Equation 9) loss are SN, MN respectively.

3.2.1 System A: Univariate Change Point

In this system, we study a univariate change point where a one-dimensional time series $\{Y_t\}_{t=1}^{60}$ stays AR(1) during time indices T_0 and AR(2) during time indices T_1 , as detailed in Equation 17. The

Model Types	Configuration	A1	A2
Fixed	AR1, w20	1.043	1.000
Model	AR1, w40	1.177	1.198
	AR2, w20	1.000	1.010
	AR2, w40	1.158	1.201
	AR3, w20	1.015	1.044
	AR3, w40	1.136	1.187
Information	AIC w20	1.030	1.063
Criterion	BIC w20	1.038	1.064
	AIC w40	1.385	1.546
	BIC w40	1.537	1.598
Adaptive	DMS-SN	1.044	1.075
Learning	DMS-MN	1.032	1.075
	DMS-Huber	1.037	1.175
	DMS-MC	1.018	1.014
	Ensemble-SN	1.015	1.041
	Ensemble-MN	1.012	1.038
	Ensemble-Huber	1.038	1.122
	Ensemble-MC	1.010	1.016

Table 2: Systems A1 and A2: average MSE results from 10000 simulated samples. A1 columns are normalised relative to AR(2), w20, and A2 columns to AR(1), w20.

forecasting horizon is set at k=3 and we evaluate the forecast at time t=60. For the AL set-up, we build $H=\{AR(1),AR(2),AR(3)\}$ each with two estimation strategies: least squared with a window size of 20 or 40. We investigate a pair of choices for (T_0,T_1) . In system A1, we set $T_0=[30]$ and $T_1=\{31,32,...,60\}$, so at the time of forecast, the DGP is an AR(2); whereas for the system A2, we set $T_0=\{31,32,...,60\}$ and $T_1=[30]$, thus the process is an AR(1) at the time of forecast.

$$Y_{t} = \begin{cases} 2 + 0.1Y_{t-1} + \varepsilon_{t} & \text{When } t \in T_{0} \\ 10 + 0.2Y_{t-1} - 0.5Y_{t-2} + \varepsilon_{t} & \text{When } t \in T_{1} \end{cases}$$
(17)

To evaluate the method of AL, we implement automatic model selection methods AIC and BIC with different window sizes. For a given information criterion, the same data window is used to evaluate the likelihood and penalisation for selection, as well as to estimate parameters for the chosen AR(p) models. There is no obvious way to determine the window size. Here, we evaluate a variety of window choices, but notice that in practice, this is not achievable a priori as neither AIC nor BIC determine the window size.

The results of the forecasts applied to the simulations A1 and A2 are reported in Table 2. By definition, in system A1 the fixed model which matches the underlying DGP most closely is AR(2) with an estimation window of 20. Unsurprisingly it outperforms all other models. A window size of 40 would include data that are part of the AR(1) regime, leading to a contaminated estimation. Likewise in system A2 the best performing fixed model is AR(1) with a window of 20.

We note that the best performing AL configuration outperforms the best information criterion in terms of the average MSE. If we also look at the average of the results for the information criterion or fixed models in Table 2, we see almost all the AL configurations outperform, implying the robustness of AL to perform under the change point. To investigate further the results, we observe the top panel in Figure 3, where the frequency of each fixed model selected by one of the top performing AL methods (DMS-MC) across the simulated samples is plotted, alongside the ones by top performing information

criteria. There is a clear ability of AL to adapt to the forecasts from the top-performing fixed models. In the case of A1 where the eventual model is AR(2) after the change point, the model is able to select it frequently, and ensure the window size is mostly 20. Likewise for the case of A2, where AR(1) is preferred as the adapted forecast. This behaviour is much stronger than in the information criteria model selection, which over-penalises the parametric models and prefers the constant model AR(0) more often.⁵

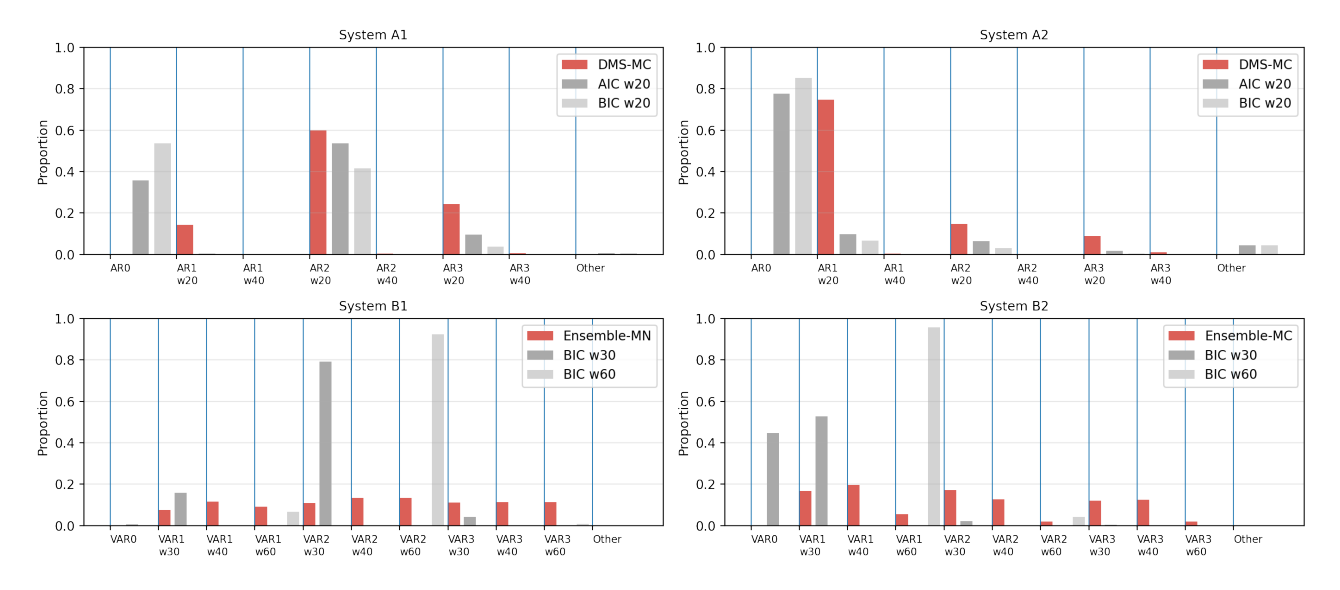


Figure 3: Summary of model selections. Top panel: system A. Bottom panel: system B. The frequency of each fixed model selected by the top performing AL method across the simulated samples, alongside the ones by top performing information criteria. In the case of Ensemble methods (bottom panel), the frequency is measured by the weight in the ensemble for each model selected.

3.2.2 System B: Multivariate Change Point

Here, we increase the dimension to a two-dimensional time series, and study a multivariate change point on $\{Y_t\}_{t=1}^{83}$. As detailed in Equation 18, $Y_t = (Y_{1,t}, Y_{2,t}) \in \mathbb{R}^2$ follows a VAR(1) at time $t \in T_0$ and elsewhere VAR(2). The forecasting exercise is to forecast $y_{1,83}$ at time 80. For the AL, we build $H = \{\text{VAR}(1), \text{VAR}(2), \text{VAR}(3)\}$ each with least squared estimations of three different window sizes: 30, 40, 60. As with system A, we investigate two cases for the change point: in system B1, we set $T_0 = [40]$ and $T_1 = \{41, 42, ..., 80\}$, and the other way around for system B2.

$$Y_{t} = \begin{cases} \begin{bmatrix} 5 \\ 0 \end{bmatrix} + \begin{bmatrix} 0.5 & 0 \\ 0 & 0.5 \end{bmatrix} Y_{t-1} + \varepsilon_{t} & \text{When } t \in T_{0} \\ \begin{bmatrix} 5 \\ 3 \end{bmatrix} + \begin{bmatrix} 0.5 & 0.6 \\ 0 & 0.5 \end{bmatrix} Y_{t-1} + \begin{bmatrix} 0 & 1 \\ 0 & 0 \end{bmatrix} Y_{t-2} + \varepsilon_{t} & \text{When } t \in T_{1} \end{cases}$$
(18)

As reported in Table 3, Ensemble models perform well, with the top ones even outperforming the best fixed models in B1. There is also an overall robustness in the AL models when comparing across other fixed models or information criteria, especially for cases like B2. The Ensemble weights do not hugely concentrate on the outperforming models or methods, as plotted in the lower panel of Figure 3: instead, it is spread out, and have some level of higher weights to the outperforming ones (VAR(2))

⁵ The AR(0) constant model is a necessary component of AIC and BIC model selection, so that the free parameters can be appropriately penalised. However, that does not make sense in the context of AL, where autoregressive terms are designed to exist.

for B1 and VAR(1) for B2). However, there are certain selection taken place: especially in B2 where w60 models perform poorly, Ensemble method is able to avoid allocating significant weights to w60 models.

Model Types	Configuration	B1	B2
Fixed	VAR1, w30	1.107	1.020
Model	VAR1, w40	1.053	1.000
	VAR1, w60	1.003	1.623
	VAR2, w30	1.072	1.095
	VAR2, w40	1.000	1.049
	VAR2, w60	1.000	1.967
	VAR3, w30	1.178	1.233
	VAR3, w40	1.053	1.129
	VAR3, w60	1.030	2.114
Information	AIC w30	1.109	1.068
Criterion	BIC w30	1.079	1.029
	AIC w60	1.012	1.878
	BIC w60	1.004	1.670
Adaptive	DMS-SN	1.079	1.167
Learning	DMS-MN	1.055	1.159
	DMS-MC	1.065	1.091
	DMS-Huber	1.061	1.220
	Ensemble-SN	0.995	1.145
	Ensemble-MN	0.991	1.120
	Ensemble-Huber	0.992	1.143
	Ensemble-MC	0.999	1.088

Table 3: Systems B1 and B2: average MSE results from 10000 simulated samples. B1 columns are normalised relative to VAR(2), w40, and B2 columns to VAR(1), w40.

3.2.3 System C: Financial Change Point

For a more financially relevant simulation, we consider the following stochastic system:

$$\frac{dS(t)}{S(t)} = \begin{cases} 0.01dt + 0.01dW(t) & \text{When } t \le t^c \\ -0.01dt + 0.1dW(t) & \text{When } t > t^c \end{cases}$$
 (19)

where $W(\cdot)$ is a standard Weiner process, and we put a step size of 1 and time index [113] for all simulated samples. S(0) is set as 15. t^c is randomly chosen from a set $\{50,70\}$ with equal probabilities. We consider the 3-step-ahead log-returns of the asset as the dependent variable: $y_t := \log(S_t) - \log(S_{t-3})$. The AL and fixed model configurations are the same as in system A. From time index 57 to 110, all models produce 3-step-ahead forecasts $\hat{y}_{t+3|t}$ and we evaluate the forecasts both statistically by MSE and Correct Sign (CS), and financially by Sharpe Ratio (SR), Annualised Return (ANR) and Maximum Drawdown (MDD). ANR and SR are key profitability evaluation metrics for financial portfolios, while MDD is a key portfolio risk evaluation metric.

These financial evaluation metrics are dependent on the deployment of a "trading strategy" which converts the forecast into an allocation of capital. The choice of trading strategy will influence the metrics reported. Here we choose a simple binary trading strategy which bets in the direction of the forecasts, the technical details of which are given in subsection A.3. Alternative constructions

		I							
Model Types	Configuration	MSE50	MSE70	CS50	CS70	SR50	SR70	MD50	MD70
Fixed	AR1, w20	3.875	3.028	0.536	0.608	0.604	0.578	-0.416	-0.379
Model	AR1, w40	3.611	2.885	0.530	0.596	0.484	0.346	-0.417	-0.394
	AR2, w20	3.908	3.050	0.534	0.605	0.597	0.573	-0.411	-0.384
	AR2, w40	3.532	2.865	0.528	0.592	0.459	0.262	-0.423	-0.405
	AR3, w20	4.543	3.446	0.529	0.601	0.543	0.518	-0.406	-0.391
	AR3, w40	3.985	3.150	0.521	0.588	0.382	0.199	-0.419	-0.415
Information	AIC w20	5.141	4.033	0.531	0.603	0.521	0.547	-0.409	-0.377
Criterion	AIC w40	4.914	4.052	0.526	0.593	0.406	0.348	-0.407	-0.391
	BIC w20	5.038	3.976	0.533	0.603	0.535	0.536	-0.414	-0.380
	BIC w40	4.883	4.052	0.527	0.593	0.419	0.332	-0.409	-0.392
Adaptive	DMS-SN	4.219	3.282	0.529	0.599	0.481	0.430	-0.405	-0.390
Learning	DMS-MN	4.237	3.299	0.530	0.600	0.479	0.453	-0.406	-0.382
	DMS-Huber	4.266	3.317	0.530	0.600	0.454	0.525	-0.417	-0.378
	DMS-MC	4.108	3.231	0.531	0.600	0.528	0.438	-0.408	-0.387
	Ensemble-SN	3.804	2.993	0.532	0.600	0.516	0.444	-0.417	-0.400
	Ensemble-MN	3.816	3.005	0.532	0.600	0.522	0.441	-0.413	-0.395
	Ensemble-Huber	3.821	3.011	0.532	0.600	0.481	0.510	-0.428	-0.390
	Ensemble-MC	3.789	2.996	0.533	0.600	0.549	0.432	-0.420	-0.397

Table 4: Systems C: average MSE, CS, and SR and median MDD results from 10000 simulated samples. SR50 refers to the mean SR when $t^c = 50$, whereas SR70 refers to the average when $t^c = 70$ and likewise for CS. MD50 and MD70 refer to the median MDD when $t^c = 50$ and 70 respectively. Columns are not normalised.

include betting in proportion to the predicted return, but this can lead to additional complexity when comparing across forecasting horizons, etc. We ignore funding and transaction costs in this trading strategy, since that is orthogonal to the evaluation of the predictive strength of the AL models. This study contributes to the general finding that financial evaluation metrics only agree with MSE up to a certain extent, and may be a better tool for model evaluation for noisy and correlated financial data.

The results are reported in Table 4. Unlike in system A and B, we now evaluate the forecast at multiple time steps in each simulation, and so there is no clear window choice that avoids contaminated data from before the change point. In terms of MSE, there is a dramatic relative improvement in the AL models over the information criterion based model selection, with this performance being robust across both $t^c = 50$ and $t^c = 70$. AL models also have less variability than fixed models in terms of performance across both change points, with the MSE of AL converging close to the best fixed model in either case.

However, when comparing against financial metrics, ambiguity arises. The average SR of our trading strategy across simulations suggests the performance of the AL and IC (information criterion) methods are very similar, with the best AL and best IC having very similar values according to each metric. The maximum drawdown is reported by its median among the samples as statistically it is an extremum estimator. Interestingly, it generally does not align with the same best-performing model as selected by the other metrics.

The financial metrics are mostly related to the direction of the forecast based on our trading strategy, hence CS provides both financial and statistical evaluation. We see that when the change point occurs later in the series at $t^c = 70$, all models are better at predicting the sign of the forecast, potentially due to reduced data contamination under that regime-switch. Table 4 also suggests the models selected by AIC and BIC are slightly better at predicting the sign of the return, particularly when the change point occurs at $t^c = 70$. This is contradictory since information criteria models were worse at predicting the magnitude of the return, hence having higher MSE.

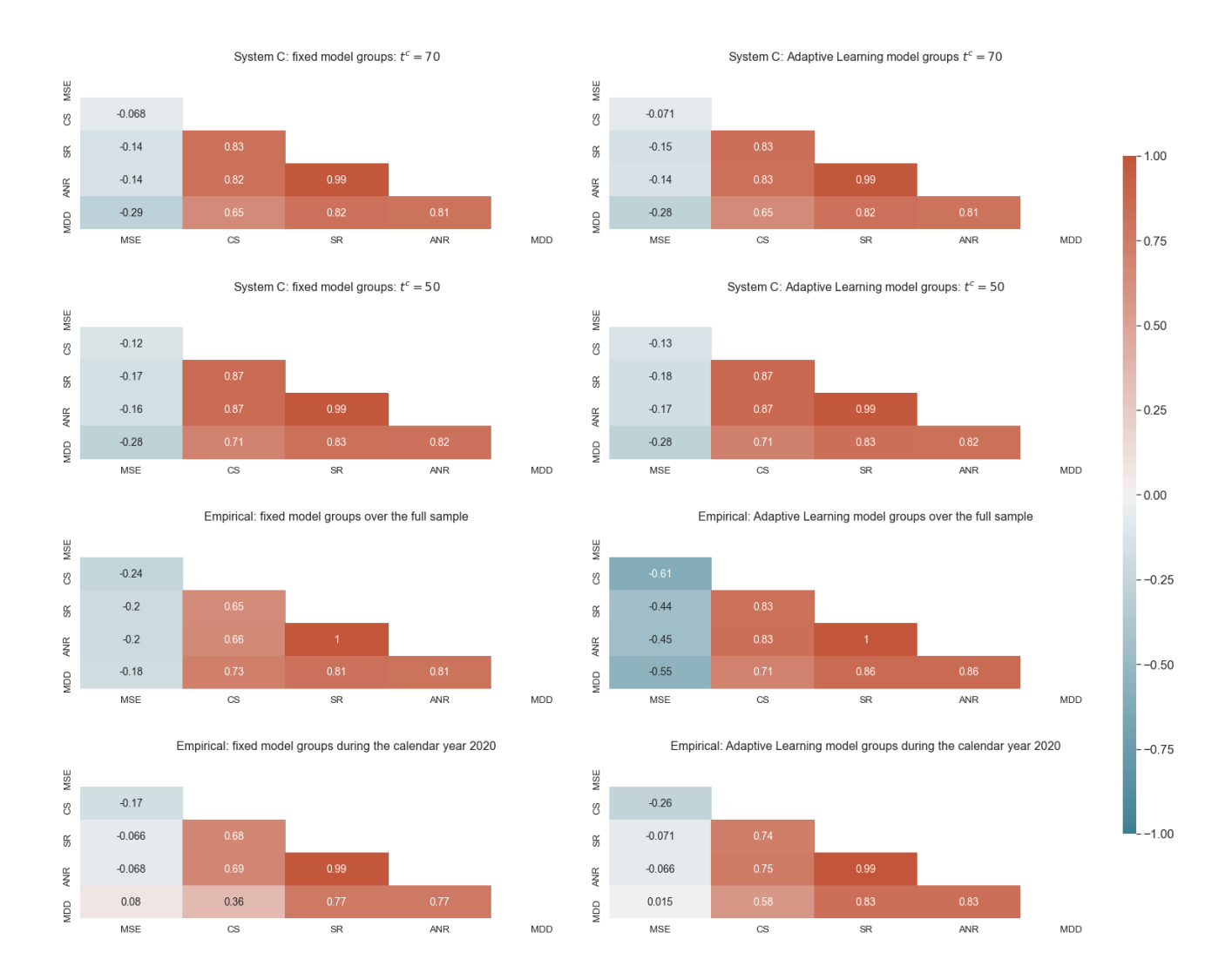


Figure 4: Correlation matrices between financial and statistical evaluation metrics. Top four: simulated system C. Bottom four: empirical data.

Motivated by this variability in the best metrics, we plot in Figure 4 the correlation matrices amongst these metrics for the simulated samples. As can be observed in the upper panels, different correlations persist, while there is no strong relationship between the MSE and other financial evaluations. As such, the correct sign of the prediction is all that will determine the financial metric evaluation, not the correct magnitude of the forecast as measure by MSE.

This is further studied in section 4, where a similar behaviour in model evaluation exists: in the lower panels of Figure 4, the same pattern is visible but it varies quite significantly across groups of models and time. In particular in 2020, when the market was more volatile and the structure varies significantly, we see weakened relationship between MSE and other metrics. For the MDD in particular, both model groups suggest a weak positive correlation, which is counter-intuitive.

4 Empirical Applications

In this section we turn our attention to an empirical study focused on predicting the returns of the major US stock market index, the S&P 500. We build on many of the techniques introduced in the previous section for the simulation studies, and extend the range of fixed models to include exogenous variables such as the VIX term structure and US Yield Curve, which have been shown in previous empirical studies to have predictive power, over certain periods, for the US stock market, as reviewed in section 1.

4.1 Models

Denote SP_t as the closing price of the S&P 500 on day t. Similar to the system C simulation, we start by defining a k-period return of SP as $y_t := \log(SP_t) - \log(SP_{t-k})$, and we study $k \in \{3, 5\}$ throughout. These forecast horizons are chosen for two reasons. Firstly, the forecast horizon cannot be too large, as naturally the noise as part of the DGP can be huge over a large forecasting horizon, especially in the presence of potential change points. Secondly, for smaller k, the number of forecasts available to be studied as part of the validation is smaller, thus failing the motivation behind the design of AL; neither would this be the interest of the empirical literature or forecasting practitioners, as short-horizon forecasts have limited applications.

As exogenous variables, the Volatility Index (VIX) and Yield Curve (YC) are studied in the following ways. We start by generating summarative slopes for VIX and YC, denoted more generally as slope_t in the rest of this section. We also consider using the short and long-run rates on the VIX and YC as individual regressors, denoted as short_t and long_t respectively. Technical details of the data availability and feature engineering are clarified in subsubsection A.4.1.

Model Group	AR Dimension and Order	Explanatory Variables	Equation
MG1	AR(p)	None	Equation 20
MG2N	Х	VIX or YC Slopes	Equation 21
MG2T	AR(p)	VIX or YC Slopes	Equation 22
MG2V	$V\!AR(2,p)$	VIX or YC Slopes	Equation 23
MG3N	×	VIX or YC Short/ Long Rates	Equation 21
MG3T	AR(p)	VIX or YC Short/ Long Rates	Equation 22
MG3V	VAR(3,p)	VIX or YC Short/ Long Rates	Equation 23
MG4V	VAR(3,p)	VIX and YC Slopes	Equation 23

Table 5: Overview of the Parametric (Fixed) Model Groups

We study a range of parametric models and estimation techniques as summarised in Table 5. MG1 is a standard AR(p) model, where we assemble the autoregressive coefficients to a p-dimensional vector $\phi_t = (\phi_{t,1}, ..., \phi_{t,p})$ and thus lagged dependent variables $z_{\tau} = (y_{\tau-1}, ..., y_{\tau-p})$, giving the estimation equation in Equation 20:

$$y_{\tau} = \alpha_t + \langle \phi_t, z_{\tau} \rangle + \varepsilon_{\tau} \quad (MG1)$$
 (20)

MG2N and MG3N, shown in Equation 21, are simple linear regression models with exogenous regressors related to the VIX Curve and the Yield Curve. Model Group 2 (MG2N) uses the slopes of the VIX and YC, whereas Model Group 3 (MG3N) uses short- and long-term maturity data from the VIX and YC. In both cases, the explanatory variables are captured by the row vector $x_{\tau-k}$. For simplicity of expression, the constant term is adjoined to the vector $x_{\tau-k}$. The dimension of the linear

⁶ See Yang (2020) and Crook et al. (2020) for examples.

coefficient β_t follows accordingly.

$$y_{\tau} = \langle \beta_t, x_{\tau - k} \rangle + \varepsilon_{\tau} \text{ where } x_{\tau - k} = \begin{cases} (1, \text{slope}_{\tau - k}) & (\text{MG2N}) \\ (1, \text{short}_{\tau - k}, \log_{\tau - k}) & (\text{MG3N}) \end{cases}$$
 (21)

The MG2T and MG3T models respectively adopt the same exogenous variables as MG2N/3N, but also include a lagged dependent variable in the regression, as shown in Equation 22. To capture lagged values of the dependent variable, we adopt the same convention as in Equation 20 by using z_{τ} to estimate lags up to an autoregressive order p.

$$y_{\tau} = \langle \beta_t, x_{\tau - k} \rangle + \langle \phi_t, z_{\tau} \rangle + \varepsilon_{\tau} \text{ where } x_{\tau - k} = \begin{cases} (1, \text{slope}_{\tau - k}) & (\text{MG2T}) \\ (1, \text{short}_{\tau - k}, \text{long}_{\tau - k}) & (\text{MG3T}) \end{cases}$$
(22)

As shown in Equation 23, MG2/3/4V represent VAR(N, p) models, where ϕ_t is a p-dimensional vector of N-dimensional matrices, since y_{τ} is N-dimensional and includes the endogenous return and the aforementioned explanatory variables.

$$y_{\tau} = \alpha_t + \langle \phi_t, z_{\tau} \rangle + \varepsilon_{\tau} \quad (MG2/3/4V)$$
 (23)

The AL configuration is as follows. The model space includes all of the above specifications and for each model in the model space we equip the OLS estimation technique with a window size of 22, 63, 126, and 252, with the exception of VAR models where we only consider window sizes that satisfy $w > N^2(2p+1)$ where p is the number of lags used in the VAR model, with variables of dimension N. At any point in time, this gives a total of 2093 models for AL model selection. The forms of learning functions are kept the same as those we studied in section 3, and we trial a range of hyperparameters, see subsubsection A.4.2.

4.2 Results

4.2.1 Overall Performance

Displayed in Table 6 are the full sample performance results when averaging within model groups for k = 3 (upper) and k = 5 (lower). In each fixed model group, the results are averaged across the individual fixed models, which vary by autoregressive order (p), the size of the estimation window (w) and the exogenous variables used. Similarly, for the AL model groups these results are averaged across all of the hyperparameters.

As a category, the AL models achieve better statistical and financial performance than the fixed models overall. For a forecast horizon k=3, the top-performing AL model groups outperform the best fixed model groups on almost every metric. For k=5, the AL models achieve performance that is close to the best of the fixed model categories, while also being much more stable.

This stability can also be seen in Figure 5, where clearly the AL models have a lower proportion of outliers with respect to MSE than the fixed model categories, while also being more robust in the most volatile years, the notable example being 2020. As a remark for model evaluation, the relationship between MSE and SR is time-varying and in many cases close to none, whereas the relationship between SR and MDD stays robust, which coincides with the overall observation as per Figure 4.

\overline{k}	Model Groups	Model Types	$1000 \times MSE$	CS	SR	$100 \times ANR$	MDD
3	Fixed	MG1	0.390	0.522	-0.268	-3.776	-0.531
	Models	MG2N	0.412	0.551	-0.107	-1.687	-0.434
		MG2T	0.552	0.532	-0.120	-1.698	-0.380
		MG2V	0.795	0.533	-0.079	-1.131	-0.350
		MG3N	0.502	0.536	0.093	1.670	-0.340
		MG3T	0.705	0.525	0.067	1.040	-0.327
		MG3V	0.758	0.532	0.090	1.372	-0.304
		MG4V	0.735	0.533	0.008	0.173	-0.322
3	Adaptive	DMS-SN	0.574	0.524	-0.234	-3.429	-0.473
	Learning	DMS-MN	0.539	0.521	-0.111	-1.535	-0.479
	Models	DMS-Huber	0.600	0.518	-0.023	-0.335	-0.423
		DMS-MC	0.398	0.532	-0.145	-2.184	-0.377
		Ensemble-SN	0.461	0.547	0.267	$\boldsymbol{4.062}$	-0.302
		Ensemble-MN	0.482	0.543	0.216	3.054	-0.328
		Ensemble-Huber	0.501	0.543	0.214	3.071	-0.315
		Ensemble-MC	0.379	0.550	0.175	2.894	-0.324
5	Fixed	MG1	0.657	0.530	-0.171	-2.416	-0.409
	Models	MG2N	0.773	0.552	-0.021	-0.238	-0.400
		MG2T	1.255	0.539	-0.017	-0.207	-0.305
		MG2V	4.746	0.544	-0.079	-1.061	-0.330
		MG3N	1.127	0.537	0.141	2.364	-0.320
		MG3T	2.185	0.529	0.086	1.333	-0.292
		MG3V	21.920	0.545	0.121	1.817	-0.283
		MG4V	3.615	0.542	0.038	0.567	-0.325
5	Adaptive	DMS-SN	1.051	0.545	0.051	0.768	-0.281
	Learning	DMS-MN	1.164	0.536	-0.147	-1.944	-0.366
	Models	DMS-Huber	1.289	0.526	-0.188	-2.464	-0.390
		DMS-MC	0.730	0.549	0.013	0.587	-0.344
		Ensemble-SN	1.225	0.544	0.184	2.698	-0.308
		Ensemble-MN	0.811	0.537	0.208	2.859	-0.278
		Ensemble-Huber	0.834	0.540	0.233	3.166	-0.274
		Ensemble-MC	0.702	0.557	0.251	3.987	-0.270

Table 6: Full sample empirical results for k=3 and k=5 averaging within model groups.

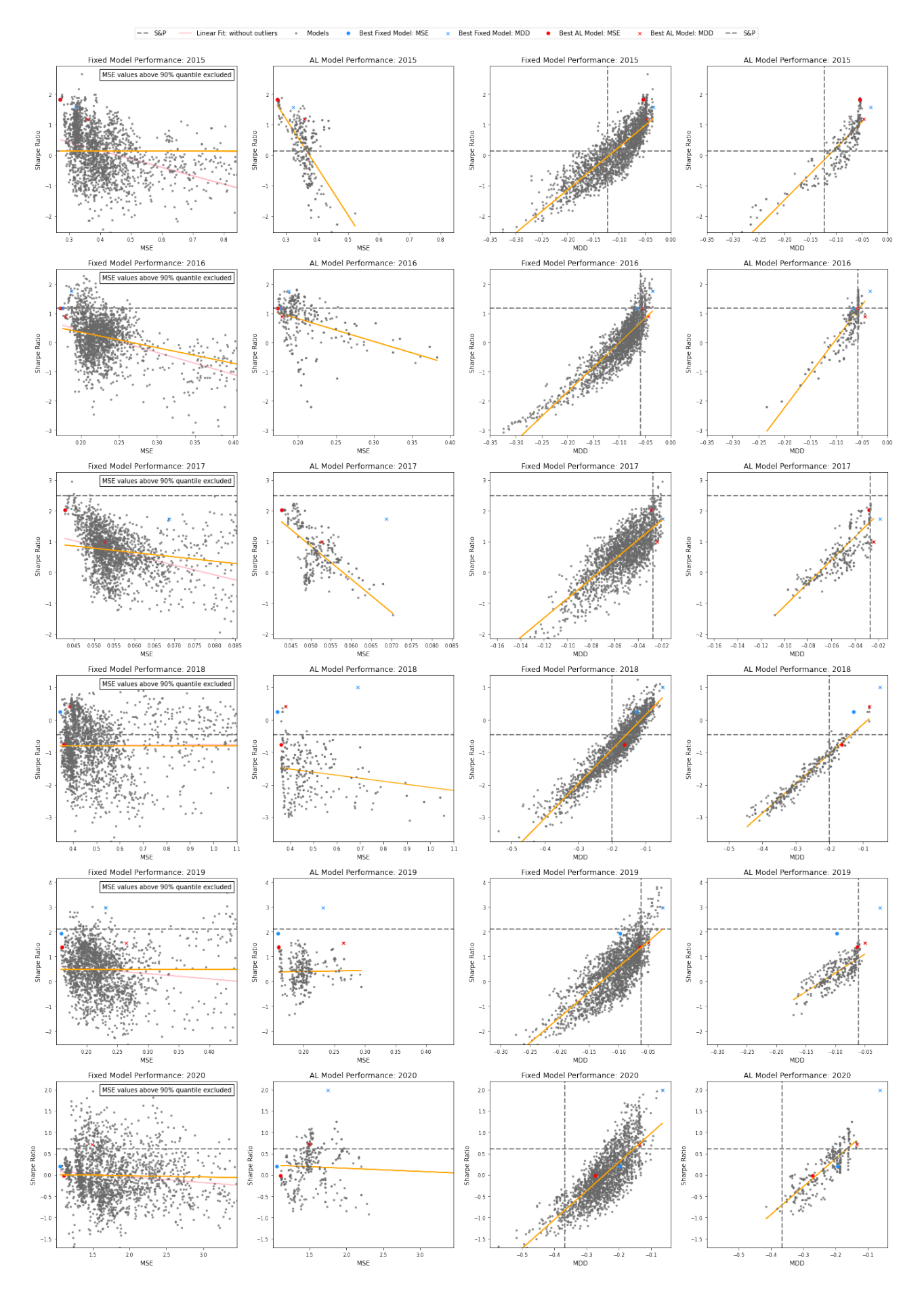


Figure 5: Year by year performance of fixed (columns 1 and 3) and AL models (columns 2 and 4) for k=3. Grey dots represent individual models rather than model categories. Colored lines represent linear fits and dotted lines represent the Long Only S&P 500 benchmark.

4.2.2 Cross-validation

One observation we can make from Figure 5 is that model performance, even allowing for time-varying parameter optimisation, is not static over time. This means that the best fixed model and the optimal AL hyperparameters can also change over time, making it difficult to select a single specification that will be optimal in all periods. This motivates the use of cross validation to assess model performance, rather than relying on averaging.

Presented in Figure 6 is a comparison of the MSE observed in the AL models (left, red) and the fixed models (right, blue) when using rolling windowed cross validation for each full year of data. This method of optimisation involves validating models on a recent tranche of data (in our case one financial year) and testing models in the subsequent period. For both AL and fixed models, we choose the best 30 models from validation, and deploy and evaluate these models in testing.

Performing this optimisation for each year, we observe consistent outperformance of the AL models when compared to the fixed models. In almost every year and across both k=3 (upper) and k=5 (lower), AL models generally obtain a lower MSE than fixed models, while also having much lower variability amongst the best models in terms of performance.

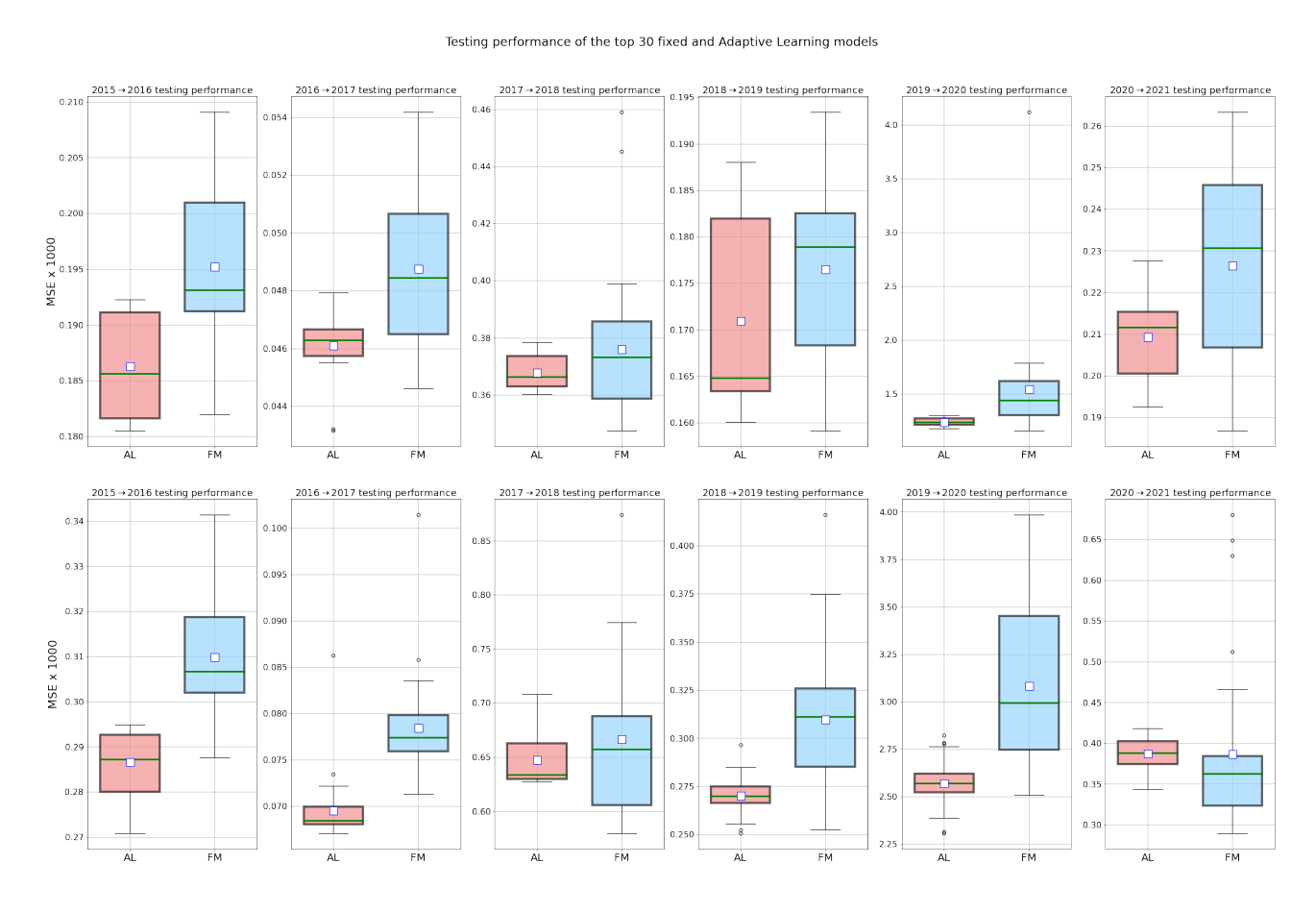


Figure 6: Year-by-year testing performance of the Adaptive Learning models (red) and fixed models (blue) using rolling windowed cross validation. For both model categories, the best 30 models from the previous year are chosen and evaluated in the testing period. Upper panel represents a forecast horizon of k = 3 and the lower panel k = 5.

4.3 Case Study: 2020 Market Crash

4.3.1 Interpretation

Another aspect of the strong performance of AL models is the robustness to volatile years, evidencing its ability to adjust model selection according to changes in DGP. In this section, we interpret the changes in AL model selection that happen before, during and after a major regime-switch in the series, and explain how parametric models may be misspecified at these times.

Figure 7 displays the testing results for the first quarter of 2020, one of the most volatile periods in the dataset. Similar to Figure 6, we choose both the AL models and fixed models based on their statistical performance (MSE) in the previous year and deploy these models in testing. In this case, however, we choose the single best model from validation and provide a more granular interpretation of its estimation and performance. Over this testing period, the best AL model from validation outperforms the best fixed model in terms of MSE by 27.3% for a forecast horizon k = 3, while for k = 5 AL outperforms by 38.7%. These results and associated financial metrics can be seen in Table 7.7

k	Type	Configuration	$1000 \times MSE$	CS	SR	$100 \times \text{ANR}$	MDD
3	AL Fixed	Ensemble-MC MG3T, AR(4), $w = 252$, VIX 3-8m	2.984 4.102	0.500 0.409	-0.958 -2.081	-51.591 -81.887	-0.220 -0.224
5	AL Fixed	Ensemble-MC MG3N, $w = 252$, VIX 3-6m	7.067 11.526	0.515 0.529	-1.415 -2.264	-70.035 -100.219	-0.214 -0.288

Table 7: 2020 Q1 testing performance of the best fixed and AL model from validation (calendar year 2019).

The upper panel of Figure 7 may explain the outperformance of the AL model relative to the fixed model. There is evidence of stability in the forecasts of the AL models, which vary less erratically and have a lower magnitude than the fixed models. Where an individual fixed model may perform well in one period, it can have high bias and thus poor performance out-of-sample, in light of time-varying distributions and heteroscedasticity. Ensembling the fixed model forecasts, while also accounting for model quality, makes the AL model less prone to large outlying forecast errors.

The problem of misfitting becomes particularly pronounced in this period due to the clear regime-switch relative to the validation data. As was discussed in subsection 3.2, fixed models with the largest window sizes may perform well in cases where the DGP is unchanging, owing to greater stability in parameter estimation. However, under conditions of regime-switching these models face the issue of data contamination, leading to an overall misfit. This underscores the problem with cross validation as applied to financial time series; it assumes that the DGP will remain constant between periods. AL gets around this problem by providing time-varying cross validation. This allows AL, for instance, to have a general preference for large window sizes but also to select models with smaller window sizes when larger ones are contaminated.

There also exists the issue of structural breaks in the fixed model parameters, which may occasionally induce very large forecasting errors for a particular fixed model. As can be seen in the bottom panels, the parameter estimates of the best fixed model were highly unstable during this period of regime switching, as a consequence of the market panic and volatility. In these situations, parameter estimates can be misleading and may even invert from their long-run relation, again strengthening the need for model averaging to ensure stability in the forecast.

 $⁽g, \Xi_g)$ takes (MG2N(VIX slope), w252) for both of the AL.



Figure 7: Comparing the best Adaptive Learning model from validation to the best fixed model from validation over the testing period. Validation period is the full year 2019, and the testing period displayed is the first quarter of 2020.

Shown in the sixth panel, the parameters of the underlying comparison used in the AL Ensemble can also be highly unstable. In this case, the model belongs to MG2N and uses VIX slope as the exogenous variable with a window size of 252. We can see that across both forecast horizons, the value of the slope parameter inverts from the value observed prior to the regime-switch and from the relationship noted elsewhere in the literature. Yet despite affecting the loss computed in those periods, AL still manages to select the constituent forecasts amongst top performing models in a stable manner (the third to the fifth panels) and hence has a greater stability relative to a single fixed model.

4.3.2 Financial Applications

In this section, we demonstrate the applicability of AL models to the domain of financial risk management by illustrating its performance during the 2020 crash. In Figure 8, we select the 10 best models by MDD from validation (2019, left) and deploy and evaluate these models in testing (Q1 2020, right). Selecting by MDD has the effect of choosing models with the strongest risk management profile, rather than rewarding models that only perform well by MSE; especially given that the relationship between financial and statistical performance metrics can be weak.

As can be seen in the left plots of the upper two panels, the best fixed models can achieve good financial performance in validation, being higher in terms of SR than AL models and having a superior MDD across both forecast horizons. However, just as in subsubsection 4.2.2 and subsubsection 4.3.1, this performance is not stable and as a category the fixed models underperform AL in testing. Shown in Table 8, we see that fixed models underperform AL on nearly every metric and across both forecast horizons. This comes again to the problem of misfitting, where we validate these models in a non-volatile period and without allowing for changes in the DGP we deploy those same fixed specifications in a highly volatile one. The misfit can lead to poor financial performance and outlying MSE values, as was the case here.

Comparing Table 7 to Table 8, we once more observe the conflict between statistical and financial performance metrics. Across both fixed models and AL, models that are chosen for having low MSE in validation again had lower MSE in testing, but were outperformed in terms of financial metrics by models chosen by MDD. This speaks firstly to the conflict between traditional and non-traditional evaluation metrics, but also to the value of SR and MDD as tools for contextual evaluation in financial time series.

Table 8 also provides an interesting observation on risk management. A long only holding strategy may be prone to large drawdowns during volatile periods. An investor who purchased the S&P 500 at the beginning of 2020 would have seen a drawdown of 36.5% in less than 3 months. In the second last panel of Figure 8, we show the losses that were incurred by the long only strategy compared to a strategy that invests equally in the 10 AL models and another that invests equally across the 10 fixed models. Clearly, fixed models can reduce losses compared to holding the Index, but even with the lower drawdown they had a poorer SR than the Index itself. AL models show more promise, having greatly improved the MDD compared to long only while at the same time having a higher SR. The bottom panel represents the implied holdings, and here we see that the strong performance of AL is attributed to the fact that AL models reacted more quickly than fixed models in adjusting their trading signals to initially be close to zero and soon after to be negative.

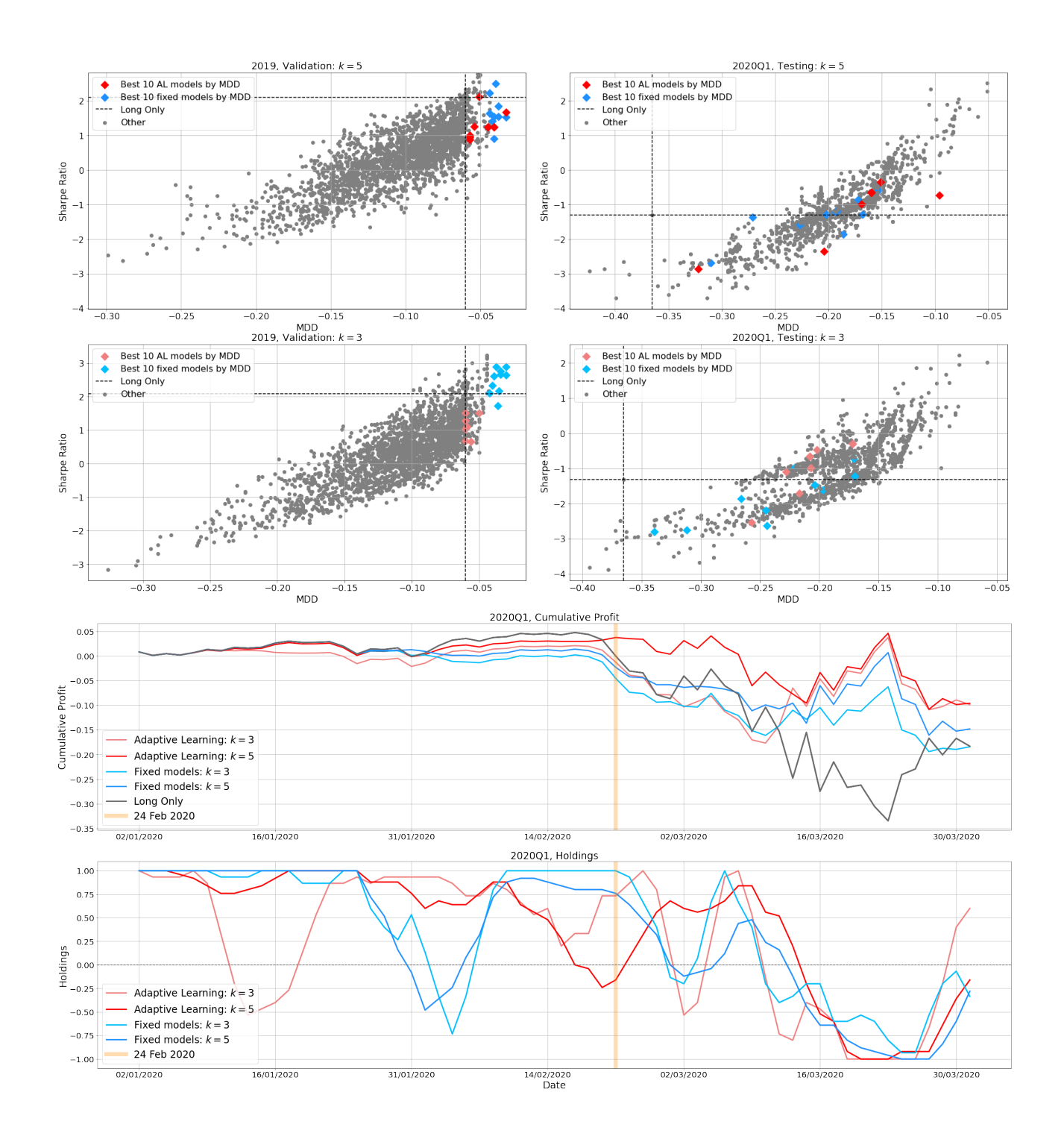


Figure 8: 2020 Q1 testing performance of AL and fixed models using MDD as the selection criterion.

\overline{k}	Model Types	$1000 \times MSE$	CS	SR	$100 \times \text{ANR}$	MDD
3	Adaptive Learning Models Fixed Models Long Only	5.305 11.953	0.447 0.468 0.530	-0.967 -1.820 -1.307	-40.107 -74.870 -74.414	-0.208 -0.237 -0.365
5	Adaptive Learning Models Fixed Models Long Only	9.583 103.417 -	0.574 0.528 0.588	-1.048 -1.391 -1.307	-38.982 -60.154 -74.414	-0.174 -0.208 -0.365

Table 8: Averaging across the 10 selected models in Figure 8. AL models obtain superior financial performance across all three metrics, and greatly reduce the drawdown compared to Long Only.

5 Discussion and Conclusion

This paper offers a formalisation of the AL method, extending from the simple frameworks first introduced in Yang (2020), and offering more generic definitions. As a method, AL sits in the field of SLT, which is concerned with inferring the functional form that maps between past input and output in a way that can be extended to unseen observations. AL is also firmly a time series method, since it pays particular attention to how this functional form may vary over time, given the natural ordering of a time series dataset.

In this way, AL can be thought of as a model selection technique, but differs from traditional ones in a number of ways. While information criteria focus on the complexity and the 'goodness-of-fit' of a particular model to in-sample data, AL offers a more forecast-centric model determination method. This becomes particularly relevant in the context of a time series dataset, where we face regime-switching, and thus contaminated data during estimation. In those cases, both the model and estimation technique (here, we studied more intimately on window size) should be determined so as to facilitate out-of-sample forecasting, and not only to optimise in-sample fit. As was shown in section 3, the out-of-sample forecasting performance of AIC and BIC may be highly subject to the window size used, which itself requires manual specification, and can not be determined a priori. AL offers automatic window size determination and can outperform information criteria under various time-varying distributions. As a remark for future research, because AL is broadly defined in subsection 2.2, the framework invites various methodological contributions in non-linear models and other statistical learning methods.

In section 4, we show that overall AL is capable of learning this time-varying functional form, achieving performance that is on par with, or even better than the best of the time-varying parametric models. Modern deep-learning methods (such as Hochreiter and Schmidhuber (1997) and Sirignano and Cont (2019)) can also help with learning the time-varying functional form, but face the limitation of interpretability. By indicating which variables and estimation techniques are preferred, AL offers a general interpretability that can inform variable selection and system design more broadly, and particularly in a time series framework. As was shown in Figure 7, AL provides temporal interpretability, allowing us to examine which estimation techniques were optimal during the periods judged to be worthy of interpretation, in our case, the 2020 market crash.

Finally, being highly applicable in the context of financial time series, AL shows promise to the field of portfolio and risk management. AL models achieved superior financial performance to fixed models under the same trading specifications, and greatly reduced losses compared to a long only strategy during the 2020 crash. A potential extension to the financial applications would be to engage more thoroughly with the practical application of AL to finance. This could mean, for instance, introducing modified loss functions that related to rolling-averaged profit and loss or SR, motivated by the fact that as observed in Figure 4, optimising for statistical performance may not always translate directly into financial performance. A more detailed statistical study on both the variety of assets and inference under different DGPs or stochastic frameworks would be the next step.

In conclusion, we provide a formal background to a time series learning method that can adapt to changes in candidate model performance and provide forecast-centric model selection. We propose two key configurations of the method, Dynamic Model Selection and Ensemble, and provide additional novel modifications to the local loss function. In our simulation studies, we demonstrate that the method can outperform traditional model selection techniques in the presence of regime-switching. In our empirical study, we provide a testbed for modern SLT by applying it to the domain of financial time series and presenting real-world financial applications of the learning results.

A Appendix

A.1 Notations

The following notations are used throughout this paper. The set of natural number $\mathbb N$ is assumed to start from 1. For a natural number n, [n] denotes the set of all natural numbers from 1 to n, that is, $[n] := \{1, 2, ..., n-1, n\}$. A sequence of white noises is written as $\{\varepsilon_{\tau}\}_{\tau \in T}$, and they are assumed to be independently and identically (iid) drawn from a normal distribution with mean 0 and variance σ^2 , noted $\varepsilon_{\tau} \stackrel{iid}{\sim} N(0, \sigma^2) \quad \forall \tau \in T$. For all simulations considered in this paper (section 3), the variance of the noise terms is set to unity. A n-dimensional simplex is defined as $\Delta(n) := \left\{x \in \mathbb{R}^n : \sum_{i \in [n]} x_i = 1, x_i \geq 0 \forall i \in [n]\right\}$. When $||\cdot||_p$ is written, it assumes $p \geq 1$, and takes the form of a function that maps from \mathbb{R}^n to \mathbb{R} with the n being specified, and $||x||_p := (\sum_{i \in [n]} x_i^p)^{1/p}$. The inner product $\langle \cdot, \cdot \rangle$ maps from $\mathbb{R}^n \times \mathbb{R}^n$ to \mathbb{R} as the dot product, that is, $\langle x, y \rangle := \sum_{i \in [n]} x_i y_i$. $\mathcal{L}^1(\mathbb{N})$ is the space of sequences where the 1-norm is finite, that is: $\mathcal{L}^1(\mathbb{N}) = \{(x_i)_{i \in \mathbb{N}} : \sum_{i \in \mathbb{N}} |x_i| < \infty \}$.

A.2 Simulation Notes

The following parameters of AL are used for simulation.

- System A1: $(\lambda = 0.95, p = 2, v = 10, v_0 = 7, (g, \Xi_q) = (AR(2), w20)).$
- System A2: $(\lambda = 0.95, p = 2, v = 10, v_0 = 7, (g, \Xi_g) = (AR(1), w20)).$
- System B1: $(\lambda = 1, p = 2, v = 10, v_0 = 7, (g, \Xi_g) = (VAR(2), w30)).$
- System B2: $(\lambda = 1, p = 2, v = 10, v_0 = 7, (q, \Xi_q) = (VAR(1), w30)).$
- System C: $(\lambda = 0.95, p = 2, v = 10, v_0 = 7, (g, \Xi_g) = (AR(2), w20)).$
- The quantile to find c in Huber is 0.5 throughout.

A.3 Financial Evaluation Methods

As a method for financial evaluation, we propose a strategy for generating trading signals on the S&P 500 Index, given in Equation 24.8 For a given model and forecast horizon k, our daily trading signal S_t is a weighted average of previous binary long/short indications obtained by our model.

$$S_t := \frac{1}{k} \times \sum_{j=0}^{k-1} \left(\mathbb{1}[\hat{y}_{t+k-j|t-j} > 0] - \mathbb{1}[\hat{y}_{t+k-j|t-j} < 0] \right)$$
 (24)

Given this trading strategy, we are able to obtain daily profit values k+1 days after we make our first forecast. Thus, we can denote the index of profit calculation as T_{π} . The daily profit resulting from a particular model-induced strategy, denoted as $PL_t := S_{t-1} \times \left(\frac{P_t - P_{t-1}}{P_{t-1}}\right)$. The cumulative profit arising from the strategy is thus $\pi_t = \sum_{\tau \in [t]} PL_{\tau}$.

Denote the last time index as T_{end} , we can use the final cumulative profit value $\pi_{T_{end}}$ to calculate Annualised Return (ANR) and Sharpe Ratio (SR) as follows:

$$ANR = \frac{252\pi_{T_{end}}}{|T_{\pi}|} \tag{25}$$

$$SR = \sqrt{252} \times \frac{Mean(\{PL_t\}_{t \in T_{\pi}})}{StDev(\{PL_t\}_{t \in T})}$$

$$\tag{26}$$

⁸ Notice that no transaction or other financing costs are being assumed as a consequence of the trading strategy.

Maximum Drawdown, MDD, measures the maximum observed loss from a peak to a trough in the value of a holding, is calculated as follows:

$$MDD = \min_{t \in T_{\pi}} \left\{ \frac{\pi_t + 1}{\max_{\tau \in [t]} \{\pi_{\tau} + 1\}} - 1 \right\}$$
 (27)

CS can be seen as a bridge between traditional statistical evaluation and profits induced by the above strategy, as it counts the number of corrected signs over the evaluation sample. In particular, with a desired index set T,

$$CS = \frac{1}{|T|} \sum_{t \in T} \mathbb{1}[sgn(y_{t+k}) = sgn(\hat{y}_{t+k|t})]$$
 (28)

Note that T_{π} starts k+1 days later T to satisfy the financial intuition behind the portfolio.

A.4 Notes for Empirical Applications

A.4.1 Data Availability and Feature Engineering

Throughout section 4, we use the following empirical data. Daily S&P 500 Index close levels were retrieved from Yahoo Finance. Daily data for this Spot VIX and VIX futures contracts were obtained directly from the Chicago Board Options Exchange, recording close prices and expiry dates for futures. The daily US treasury rates with constant maturity of one month, three months, six months, one year, two years, three years, five years, seven years, ten years, twenty years and thirty years are obtained from the Federal Reserve Bank of St. Louis' online database. Rates are given in percentage points and are not seasonally adjusted, calculated via the most recently auctioned bills and notes. Our full dataset spans from 2 January 2013 to 28 May 2021, with a total of 2117 observations. When referencing "full sample results" in the main text, we are referring to the evaluation period from the 13 August 2014 to 28 Apr 2021. This differs from the full dataset because initial observations are designated for training and at the latter end observations are designated for validation of the forecasts, hence truncating the dataset.

As employed in Fassas and Hourvouliades (2019), for all trading days t in our dataset, let β_t^{VIX} be the slope of the VIX term structure, as estimated via least-squares in

$$FVIX_{i,t} = \alpha_t^{VIX} + \beta_t^{VIX} M_{i,t}^{VIX} + \varepsilon_t^{VIX}$$
(29)

where $\text{FVIX}_{i,t}$ is the closing price and $M_{i,t}^{\text{VIX}}$ is the time to maturity in calendar days of the i^{th} open VIX futures contract on day t. Let $i \in \mathbf{I}_t$, $\mathbf{I}_t \subseteq \{0, 1, ..., 9\}$, where there are up to nine openly tradeable contracts on any given day. i = 0 represents Spot VIX, which is considered as the price of VIX with zero maturity.

Similarly, let β_t^{YC} be the slope of the Yield Curve, also fitted with least-squares via

$$YC_{j,t} = \alpha_t^{YC} + \beta_t^{YC} M_{j,t}^{YC} + \varepsilon_t^{YC}$$
(30)

where $YC_{j,t}$ is the rate and $M_{j,t}^{YC}$ is the time to maturity in calendar days for the respective item j on day t. $j \in \{0, 1, ..., 7\}$, representing the daily US treasury rates with constant maturity from three months up to ten years.

Alongside both the slopes of the VIX and Yield Curve, we also use short- and long-term rates for the VIX Curve and the Yield Curve as respective regressors in MG3 Model Groups. We classify the VIX Curve's short-term rates as the raw Spot, front month, second month and third month futures contracts, with all subsequent months labeled as long-term rates. Similarly, short-term rates for the Yield Curve are the one month, three months, six months, one year and two year constant maturity rates, with all other rates considered long-term.

A.4.2 Hyperparameters for AL

The choices of the hyperparameters for AL are illustrated below:

- $\lambda \in \{0.9, 0.95, 0.96, 0.97, 0.98, 0.99, 1\}$
- $p \in \{1, 2\}, v = 100, v_0 \in \{25, 50, 75\}$
- The quantile to find c is selected from $\{0.5, 0.75\}$
- (g, Ξ_q) takes two possible values: (AR(1), w252) and (MG2N(VIX slope), w252)

References

- Akaike, Hirotugu (1974). "A new look at the statistical model identification." In: *IEEE Transactions on Automatic Control* 19.6, pp. 716–723. DOI: 10.1109/TAC.1974.1100705.
- Benhamou, Eric, David Saltiel, Beatrice Guez, and Nicolas Paris (2019). "Testing Sharpe ratio: luck or skill?" In: eprint: 1905.08042.
- Coulombe, Philippe Goulet (2020). "The Macroeconomy as a Random Forest." In: eprint: arXiv: 2006.12724.
- Coulombe, Philippe Goulet, Maxime Leroux, Dalibor Stevanovic, and Stéphane Surprenant (2020). "How is Machine Learning Useful for Macroeconomic Forecasting?" In: eprint: arXiv:2008.12477.
- Crook, Oliver M., Mihai Cucuringu, Tim Hurst, Carola-Bibiane Schönlieb, Matthew Thorpe, and Konstantinos C. Zygalakis (2020). "A Linear Transportation L^P Distance for Pattern Recognition." In: eprint: arXiv:2009.11262.
- De Pace, Pierangelo (2013). "Gross Domestic Product Growth Predictions through the Yield Spread: Time-Variation and Structural Breaks." In: *International Journal of Finance & Economics* 18.1, pp. 1–24. DOI: 10.1002/ijfe.453.
- Estrella, Arturo and Frederic S Mishkin (1996). "The yield curve as a predictor of US recessions." In: Current issues in economics and finance 2.7.
- Fassas, Athanasios (2012). "The Relationship between VIX Futures Term Structure and S&P500 Returns." In: Review of Futures Markets 20, p. 299. DOI: 10.2139/ssrn.2841384.
- Fassas, Athanasios P. and Nikolas Hourvouliades (2019). "VIX Futures as a Market Timing Indicator." In: Journal of Risk and Financial Management 12.3. ISSN: 1911-8074.
- Harvey, Andrew C (2013). Dynamic models for Volatility and Heavy Tails. Cambridge University Press.
- Hochreiter, Sepp and Jurgen Schmidhuber (1997). "Long Short-term Memory." In: *Neural computation*, pp. 1735–80. DOI: 10.1162/neco.1997.9.8.1735.
- Huber, P. J. and E.M. Ronchetti (2009). Robust Statistics. John Wiley & Sons.
- Liu, Haoyang, Chao Gao, and Richard J. Samworth (2021). "Minimax rates in sparse, high-dimensional change point detection." In: *The Annals of Statistics* 49.2, pp. 1081 –1112. DOI: 10.1214/20-A0S1994.
- Lo, Andrew W. (2002). "The Statistics of Sharpe Ratios." In: Financial Analysts Journal 58.4, pp. 36–52.
- Ostmann, F and C Dorobantu (2021). "AI in financial services." In: *The Alan Turing Institute*. DOI: 10.5281/zenodo.4916041.
- Schwarz, Gideon (1978). "Estimating the Dimension of a Model." In: *The Annals of Statistics* 6.2, pp. 461 –464. DOI: 10.1214/aos/1176344136.

- Shumway, Robert and David Stoffer (2017). Time Series Analysis and Its Applications. 4th ed. Springer.
- Sirignano, Justin and Rama Cont (2019). "Universal features of price formation in financial markets: perspectives from deep learning." In: *Quantitative Finance* 19.9, pp. 1449–1459. DOI: 10.1080/14697688.2019.1622295.
- Spokoiny, Vladimir (2017). "Penalized maximum likelihood estimation and effective dimension." In: Annales de l'Institut Henri Poincaré, Probabilités et Statistiques 53.1, pp. 389–429.
- Taylor, James and Keming Yu (2016). "Using auto-regressive logit models to forecast the exceedance probability for financial risk management." In: Journal of the Royal Statistical Society: Series A (Statistics in Society) 179.4, pp. 1069–1092. DOI: 10.1111/rssa.12176.
- Yang, Parley Ruogu (2020). "Using the yield curve to forecast economic growth." In: *Journal of Forecasting* 39.7, pp. 1057–1080. DOI: 10.1002/for.2676.
- (2021). "Forecasting high-frequency financial time series: an adaptive learning approach with the order book data." In: eprint: arXiv:2103.00264.
- Yang, Yuhong (2007). "Consistency of cross validation for comparing regression procedures." In: *The Annals of Statistics* 35.6, pp. 2450 –2473. DOI: 10.1214/009053607000000514.
- Zou, Changliang, Guanghui Wang, and Runze Li (2020). "Consistent selection of the number of change-points via sample-splitting." In: *The Annals of Statistics* 48.1, pp. 413–439. DOI: 10.1214/19-AOS1814.